

Lawrence Berkeley National Laboratory

Recent Work

Title

PHOTO-MESONS FROM CARBON

Permalink

<https://escholarship.org/uc/item/3k42p73j>

Authors

Peterson, J .M.

Gilbert, W.S.

White, R.S.

Publication Date

1950-10-16

UCRL 703-Rev.
UNCLASSIFIED

UNIVERSITY OF
CALIFORNIA

*Radiation
Laboratory*

TWO-WEEK LOAN COPY

*This is a Library Circulating Copy
which may be borrowed for two weeks.
For a personal retention copy, call
Tech. Info. Division, Ext. 5545*

BERKELEY, CALIFORNIA

DISCLAIMER

This document was prepared as an account of work sponsored by the United States Government. While this document is believed to contain correct information, neither the United States Government nor any agency thereof, nor the Regents of the University of California, nor any of their employees, makes any warranty, express or implied, or assumes any legal responsibility for the accuracy, completeness, or usefulness of any information, apparatus, product, or process disclosed, or represents that its use would not infringe privately owned rights. Reference herein to any specific commercial product, process, or service by its trade name, trademark, manufacturer, or otherwise, does not necessarily constitute or imply its endorsement, recommendation, or favoring by the United States Government or any agency thereof, or the Regents of the University of California. The views and opinions of authors expressed herein do not necessarily state or reflect those of the United States Government or any agency thereof or the Regents of the University of California.

UCRL-703 Rev.
Unclassified Distribution

UNIVERSITY OF CALIFORNIA

Radiation Laboratory

Contract No. W-7405-eng-48

PHOTO-MESONS FROM CARBON

J. M. Peterson, W. S. Gilbert, and R. S. White

October 16, 1950

Berkeley, California

<u>INSTALLATION</u>	<u>Number of Copies</u>
Argonne National Laboratory	8
Armed Forces Special Weapons Project	1
Atomic Energy Commission - Washington	2
Battelle Memorial Institute	1
Erush Beryllium Company	1
Brookhaven National Laboratory	4
Bureau of Medicine and Surgery	1
Bureau of Ships	1
Carbide and Carbon Chemicals Division (K-25 Plant)	4
Carbide and Carbon Chemicals Division (Y-12 Plant)	4
Chicago Operations Office	1
Columbia University (J. K. Dunning)	1
Columbia University (G. Failla)	1
Dow Chemical Company	1
H. K. Ferguson Company	1
General Electric Company, Richland	3
Harshaw Chemical Corporation	1
Idaho Operations Office	1
Iowa State College	2
Kansas City Operations Branch	1
Kellex Corporation	2
Knolls Atomic Power Laboratory	4
Los Alamos Scientific Laboratory	3
Mallinckrodt Chemical Works	1
Massachusetts Institute of Technology (A. Gaudin)	1
Massachusetts Institute of Technology (A. R. Kaufmann)	1
Mound Laboratory	3
National Advisory Committee for Aeronautics	1
National Bureau of Standards	3
Naval Medical Research Institute	1
Naval Radiological Defense Laboratory	2
New Brunswick Laboratory	1
New York Operations Office	3
North American Aviation, Inc.	1
Oak Ridge National Laboratory	8
Patent Branch - Washington	1
Rand Corporation	1
Sandia Corporation	2
Santa Fe Operations Office	2
Sylvania Electric Products, Inc.	1
Technical Information Division (Oak Ridge)	15
Armament Division, Deputy for Research and Development (Capt. Glenn Davis)	1
Assistant for Atomic Energy, Deputy Chief of Staff (Col. Robert E. Greer)	1
Chief of Documents and Disseminations Branch (Col. J. E. Mallory)	1
USAF Assistant for Research Director of Research and Development, Deputy Chief of Staff (Col. B. G. Holzman)	1

<u>INSTALLATION</u>	<u>Number of Copies</u>
Electronic Systems Division (Mr. E. C. Trafton)	1
Chief of Scientific Advisors (Dr. Theodore von Karman)	1
USAF, Eglin Air Force Base (Major A. C. Field)	1
USAF, Kirtland Air Force Base (Col. Marcus F. Cooper)	1
USAF, Maxwell Air Force Base (Col. F. N. Moyers)	1
USAF, NEPA Office	2
USAF, Offutt Air Force Base (Col. H. R. Sullivan, Jr.)	1
USAF Surgeon General, Medical Research Division (Col. A. P. Gagge)	1
USAF, Wright-Patterson Air Force Base (Rodney Nudenberg)	1
U. S. Army, Atomic Energy Branch (Lt. Col. A. W. Betts)	1
U. S. Army, Army Field Forces (Captain James Kerr)	1
U. S. Army, Commanding General, Chemical Corps Technical Command (Col. John A. MacLaughlin thru Mrs. Georgia S. Benjamin)	1
U. S. Army, Chief of Ordnance (Lt. Col. A. R. Del Campo)	1
U. S. Army, Commanding Officer, Watertown Arsenal (Col. Carroll H. Deitrick)	1
U. S. Army, Director of Operations Research (Dr. Ellis Johnson)	1
U. S. Army, Office of Engineers (Allen O'Leary)	1
U. S. Army, Office of the Chief Signal Officer (Curtis T. Clayton thru Maj. George C. Hunt)	1
U. S. Army, Office of the Surgeon General (Col. W. S. Stone)	1
U. S. Geological Survey (T. B. Nolan)	2
U. S. Public Health Service	1
University of California at Los Angeles	1
University of California Radiation Laboratory	5
University of Rochester	2
University of Washington	1
Western Reserve University	2
Westinghouse Electric Company	4
R. F. Bacher, California Institute of Technology)	1
Cornell University	1
Total	140

Information Division
 Radiation Laboratory
 Univ. of California
 Berkeley, California

-3-

PHOTO-MESONS FROM CARBON

J. M. Peterson, W. S. Gilbert, and R. S. White

Radiation Laboratory, Department of Physics
University of California
Berkeley, California

October 16, 1950

Abstract

Photons from the Berkeley 322 Mev electron synchrotron have been used to produce mesons from a carbon target. These mesons have been observed with nuclear emulsions at angles of 45° , 90° , and 135° to the photon beam. The ratio of the number of π^- to π^+ mesons produced is 1.29 ± 0.22 , 1.30 ± 0.12 , and 1.34 ± 0.20 , respectively, at each of the above angles. The energy spectra and the differential cross sections of π mesons at each of these angles have been obtained. The total cross section for the production of π mesons is $4.0 \pm 1.6 \times 10^{-28}$ cm² per nucleus per "equivalent quantum." The number of "equivalent quanta," Q_e , is defined as the total energy in the beam divided by the maximum photon energy. The cross section for production of μ meson pairs at the target is estimated to be less than 2 percent of the cross section for π meson production.

PHOTO-MESONS FROM CARBON

J. M. Peterson, W. S. Gilbert, and R. S. White

Radiation Laboratory, Department of Physics
University of California
Berkeley, California

October 16, 1950

I. INTRODUCTION

The production of mesons by photons was definitely established for the first time when they were observed in the x-ray beam of the 322 Mev electron synchrotron at the University of California Radiation Laboratory by McMillan and Peterson¹ in January, 1949. Carbon was the first pure target material to be bombarded by the x-ray beam for the production of mesons.² Carbon was chosen because of its relatively low atomic number and its ready availability and ease of fabrication. The background is due largely to electrons, positrons, and photons that are produced and scattered in the target material and which tend to fog the nuclear emulsions used as detectors in this experiment. Since the electron pair production cross section varies as the second power of the atomic number while meson production varies by about the two-thirds power,³ the background is reduced by going to as low an atomic number as possible.

For pure photon-nucleon interactions the ideal targets to bombard with photons are either protons or neutrons. Ordinary hydrogen is perfect for the former, and deuterium is the nearest experimental approach to the latter.

¹ E. M. McMillan and J. M. Peterson, *Science* 109, 438 (1949)

² E. M. McMillan, J. M. Peterson, and R. S. White, *Science* 110, 579 (1950)

³ R. F. Mozely, *Phys. Rev.* (to be published)

Experiments using hydrogen have been done by Cook⁴ and by Steinberger and Bishop.⁵ An experiment with deuterium is now in progress.

Although it was realized that with a carbon target one might not get a true picture of a pure photon-nucleon interaction because of possible distortion by the other nucleons in a carbon nucleus, it was felt that one might get a first approximation. Also if distortion by the neighboring nucleons were important, it could be measured by comparison of the negative and positive meson spectra from carbon with those from hydrogen and deuterium. Furthermore, the energy spectra and the ratio of negative to positive mesons from carbon are each of interest per se.

An exploratory experiment² using a line target of carbon had given a rough energy spectrum of mesons emitted near 90° to the beam direction in the laboratory system. It had indicated that the angular distribution of mesons was approximately spherically symmetric, at least in the region near 90° , and also that more π^- mesons are produced than π^+ mesons by a ratio of 1.7 ± 0.2 . The present experiment was designed to display more fully the angular and energy spectrum of mesons produced in carbon by x-rays generated by 322 Mev electrons.

II. EXPERIMENTAL METHOD

The x-rays were produced in the Berkeley synchrotron by letting the 322 ± 5 Mev electron beam strike a 0.020 inch platinum target placed on the inner side of the accelerating tube. The resultant bremsstrahlung beam emerged from the machine in a narrow cone whose full width at half intensity was 0.0135 radian (0.77 degree). At 55 inches from the platinum

⁴ L. J. Cook, private communication

⁵ J. Steinberger and A. S. Bishop, Phys. Rev. 78, 494 (1950)

target the beam was collimated by a tapered hole in a lead block six inches thick as illustrated in Fig. 1. The collimating hole was 0.50 inch in diameter at the entrance end and was part of a cone whose apex was at the platinum target. This primary collimator defined by geometry a cone of x-rays whose full width was 0.0091 radian (0.52 degree). Directly behind the primary collimator was the secondary collimator, a three inch thickness of lead in which there was a cylindrical hole just slightly larger than the geometrically defined beam. The purpose of the secondary collimator was to shield the detection equipment from the spray of electrons, positrons, and secondary photons produced in the walls of the primary collimator. Cross section views of the collimator, target, and detector assembly are shown in Fig. 2 and a photograph of the experimental arrangement in Fig. 3.

The diameter of the carbon sphere was 0.620 inch, just equal to the diameter of the diverging x-ray beam at that point. That the beam size was accurately determined by geometry was confirmed by photographic film measurements. The carbon target was surrounded by a large cylinder of copper, in which were imbedded stacks of nuclear emulsion plates. Mesons emitted from the carbon were slowed down and stopped throughout a large volume of the copper, and the imbedded emulsions served to sample the meson density at various points. Both the energies and angles of the emitted mesons were determined by the positions of the meson-endings relative to the target - to within uncertainties due to scattering and to the finite size of the target.

The intensity of the x-ray beam was practically constant as it traversed the carbon target. The part of the beam which traversed the diameter of the carbon was attenuated by only 3.5 percent. Some fifteen feet beyond the carbon target the x-ray beam struck a large ionization chamber which served as the

monitor in this experiment. The considerations which went into the design of the component parts of the experiment are discussed in more detail in the following sections.

A. Detectors

Up to now, the emulsion method of detection is the only reliable method for detection of both π^- and π^+ mesons, although successful electronic techniques have been developed for the detection of π^+ mesons.^{6,7} Furthermore, the emulsion method allows one to collect at no extra cost other interesting data, such as, for example, the energy and angular distributions of μ^+ mesons. The Ilford type C-2 emulsion was chosen because its sensitivity was felt to be optimum for the identification of meson tracks and yet great enough to allow easy recognition of relatively faint μ^+ tracks at the end of the π^+ tracks. Electrons passing through this emulsion leave developable grains at only a relatively few points along its path--so few that an electron track cannot normally be recognized. These grains form a single-grain background in the emulsions and were the determining factor in the amount of exposure which could be used in this experiment. The emulsions used were nominally 100 microns in thickness.

B. Absorbers

Since the meson density drops off as the inverse square of the distance from a point target, a relatively dense material such as copper or lead was desirable as the absorbing material. The r.m.s. angle of multiple Coulomb scattering from its initial direction to the point where a meson is first detected in the emulsion can be up to 47° for a lead absorber and up to 26°

⁶ L. W. Alvarez, A. Longacre, V. G. Ogren, and R. E. Thomas, Phys. Rev. 77, 752 (1950)

⁷ J. Steinberger and A. S. Bishop, Phys. Rev. 78, 493 (1950)

for copper. Since most of the scattering takes place in the last part of the meson's trajectory, which usually is in glass, the r.m.s. angle of scatter for a typical meson is 24° for a lead absorber and 18° for copper. Because of its greater stopping power per unit thickness and because of its smaller scattering, copper was selected for the absorber material.

Since the scattering in the copper absorber is fairly large, it was decided to use completely poor geometry in the meson detection system. The large copper cylinder surrounding the carbon target as shown in Figs. 2 and 3 satisfies this condition.

Throughout the experiment the distribution in ϕ , the azimuthal angle about the x-ray beam axis, is treated as constant because the x-ray beam is unpolarized.

As indicated in Figs. 2 and 3 there were 14 slots in the outer edge of the copper cylinder cut radial to the x-ray beam axis. In these slots were placed copper boxes containing stacks of nuclear plates. Each box had space for 3 stacks of plates placed end to end, each stack containing about 14 plates. The plates were oriented so that the planes of the emulsions were approximately radial. Only the central 6 plates were selected for scanning. This geometry and selection of plates allowed one to calculate what fraction of each meson's range was in copper and what fraction in glass and emulsion. In addition, the removal of a portion of the detectors at several times during a run, allowed a variety of exposures under well controlled conditions and was economical with respect to synchrotron operating time. The difference in copper absorber thickness between consecutive plate positions was $1/3$ inch. Since the stopping power of an inch of the glass used was just slightly greater than $1/3$ inch of copper in this energy range, the whole meson energy spectrum could be

observed above a minimum energy determined by self-absorption in the carbon target.

C. Target

The spherical shape of the target was chosen as an approximation to a point source of mesons so as to afford sufficient angular resolution in the detection of the mesons. Also, this shape allows the source to have the same appearance and characteristics in all directions of observation.

The size of the carbon target was determined by the minimum detectable meson energy which was compatible with a reasonable exposure time. With the 0.620 inch diameter carbon target used, the minimum energy was 12.5 Mev.

The angular resolution of this experiment was determined not only by the scattering in the absorbing materials, but also by the angular width of the meson source as seen from the detector and by the width of the detector as seen from the source. In most cases the width of the scanned areas of emulsion was about equal to the width of the meson source, so that these two sources of angular width have approximately equal effects. The r.m.s. value of this angular width from both sources varied from about ± 5.6 to ± 1.9 degrees over the energy range at $\theta = 90^\circ$ and about ± 3.9 to ± 1.6 degrees at 45° and at 135° . Because of multiple Coulomb scattering the angle between the direction of the meson as it leaves the target and the line drawn from the end point of the meson to the target can be up to 5° . Combining these angular uncertainties one finds that the total root mean square angular uncertainties are about ± 7 degrees at $\theta = 90^\circ$ and about ± 6 degrees at 45° and 135° . The scattering calculations were made using the method developed by Foldy.⁸

⁸ L. L. Foldy, Phys. Rev. 75, 311 (1949)

The energy resolution can be affected by several factors: thickness of the target, scattering in the absorber, widths of the target and of the scanned areas, and straggling due to energy loss fluctuations. At 90° the only important factor is target thickness, and the r.m.s. energy uncertainty is a maximum of ± 4.0 Mev at the lowest energy observed and when calculated for the middle points of the various plates varies from ± 2.8 Mev down to ± 1.2 Mev at the highest energy observed. At 45° and 135° the edge of the copper absorber is at an angle of 45° to the meson trajectory, and as a result uncertainties due to scattering in the absorber and to widths of the target and scanned areas also become important. The resultant total r.m.s. energy uncertainty at 45° and 135° , again calculated for the middle points of the plates, is a maximum of ± 7.0 Mev at a meson energy of 150 Mev and decreases to ± 3.0 Mev at 33 Mev, the nominal energy at the middle of the plates of the first box.

D. Exposures

Three sets of plates were removed from the apparatus and replaced with blank plates during the exposure run. These removals occurred at exposures of 2.4, 4.8 and 9.6×10^{11} "equivalent quanta." The number of "equivalent quanta," Q , is defined as the total energy in the beam divided by the maximum photon energy. The middle exposure was about optimum. Most of the plates scanned were from this batch. The exposure was limited by the darkening of the leading edges of the plates in the box with no absorber, even though this box was about twice as far from the target as the box in the next higher energy interval.

E. Examination of the Emulsions

The emulsions were scanned for meson endings with standard microscopes of from 250 to 900 power magnification. Altogether about 84 square centimeters

-11-

of emulsion were scanned.

Meson track endings in Ilford C-2 emulsions have in general two characteristics by which they can be recognized. One is a large amount of small angle scattering over the last one or two hundred microns of the track length. The other is a relatively fast change of grain density over the last 100 microns of the track length. In addition, some types of mesons have characteristic track endings which make identification easier. It is known from data on magnetically sorted π^- mesons that about 73 ± 2 percent of the π^- mesons which stop in Ilford C-2 emulsions have one or more observable tracks leaving the meson ending.⁹ These mesons are labelled σ mesons (star mesons). Any meson track with no observable track leaving its ending is called a ρ meson. As several thousand π^- meson endings in emulsions have been observed without conclusive evidence of a $\pi-\mu$ ending,¹⁰ one can draw the conclusion that a π^- meson is almost always captured before having time to decay. Therefore, any $\pi-\mu$ decay observed in the emulsion must certainly have been initiated by a π^+ meson. From work with magnetically sorted π^+ mesons it has been observed that more than 99 percent of the π^+ mesons decay into μ^+ mesons.¹¹

The characteristics of the track endings of μ^- mesons are not as well known. From observations with cosmic ray mesons, Chang¹² has found no certain stars at the end of over 50 μ^- mesons. Other observers,¹³ using artificially produced mesons have found some 28 events in emulsions thought to be the endings of μ^- mesons. Of these, 26 are ρ -endings, and 2 are σ -types. These

⁹ F. L. Adelman and S. B. Jones, Science 111, 226 (1950)

¹⁰ University of California Radiation Laboratory Film Group, private communication

¹¹ F. M. Smith, private communication

¹² W. Y. Chang, Rev. Mod. Phys. 21, 166 (1949)

¹³ S. B. Jones and R. S. White (to be published)

-12-

2 σ -endings could have been due to π^- meson contamination.

The track ending of a μ^+ meson is always a ρ -type because it can only spontaneously decay.¹⁴ Ilford C-2 emulsions are not sensitive enough to detect electron tracks.

The types of track endings of the four kinds of mesons can be summarized in the following table:

TABLE I
Types of Meson Track Endings

Kind of Meson	Types of Endings
Negative π	σ_n, ρ ($n = 1, 2, 3, \dots$ = number of prongs)
Negative μ	ρ
Positive π	$\pi-\mu$
Positive μ	ρ

There is the possibility that a $\pi-\mu$ ending, with the μ^+ track of less than 100 microns in length, might be confused with a σ_1 -ending whose one prong is a lightly ionizing track. However, in a study of 65 σ_1 -endings in emulsions exposed to magnetically sorted π^- mesons it was found that most of the σ_1 -endings with fast prongs had also recognizable "clubs," i.e., blobs of grains at the meson endings due presumably to recoil of the residual nuclei. It is known that $\pi-\mu$ endings do not exhibit such "clubs." From these data one can deduce that only about 1 percent of all σ -endings are confusable with $\pi-\mu$ endings, provided one examines these tracks for "clubs."

From the discussion above one can interpret the various meson-track endings in the following way:

¹⁴ R. B. Leighton, C. D. Anderson, and A. Seriff, Phys. Rev. 75, 1136 (1949)

-13-

- (a) The number of π^- mesons is equal to 1/0.73 of the total number of σ meson endings.
- (b) The number of π^+ mesons is equal to the number of $\pi-\mu$ endings.
- (c) The ρ -endings are made up of 0.27 of the π^- meson endings, and also of μ^+ -endings from the $\pi-\mu$ decay processes. Since the range of the μ^+ meson is only about 600 microns, there should be, on the average, as many μ^+ -endings as π^+ -endings in any sample volume. However, not as many of the μ^+ -endings will be recognized partly because, being emitted isotropically from the end of π^+ mesons, many of them will be traveling at unfavorable angles for observation whereas most of the π^+ mesons are parallel to the plane of the emulsion. Also since the μ^+ -track on the end of a π^+ -track acts like a label, the μ^+ -ending is harder to recognize especially if short, as it has no such label. The number of μ mesons, if any, either negative or positive, emitted from the carbon target is very small. A previous experiment put an upper limit on the cross section for the production of pairs of μ mesons as 0.02 ± 0.02 of the cross section for the production of π^+ mesons and π^- mesons.¹⁵ This experiment allows a similar estimate to be made, as will be shown later. Only a negligible number of μ mesons are expected from $\pi-\mu$ decay processes in flight.

Meson endings which occur very near either surface of the emulsion are in danger of misinterpretation by an observer because lightly ionizing tracks might leave the emulsion without being recognized. To avoid these misinterpretations only meson endings 3 microns or greater from either surface after development were used in the calculations. This 3 micron criterion was established by plotting the frequency of each type of meson versus the distance to the nearest surface as is shown in Fig. 4. Since the 100 micron emulsion is

¹⁵ E. M. McMillan, J. M. Peterson, and R. S. White, unpublished data

-14-

only about 40 microns in thickness after development, the above criterion removes about 15 percent of the available emulsion volume.

The reliable observation of mesons in emulsions requires considerable experience. The absolute efficiency for the recognition of mesons by the five observers who worked on this experiment was determined by duplicate scanning of certain areas of the emulsion. All had efficiencies of greater than 90 percent for the recognition of σ and π - μ endings and greater than 80 percent for the recognition of ρ -endings. As another means of comparing the observers and minimizing their differences, each area of emulsion to be scanned was divided into three parallel sections which were generally scanned by three different observers. The results of the three sections were plotted separately and found to be consistent within the limits of random sampling. After demonstrating in this way that no significant errors would be caused by individual observer differences, the data were collected irrespective of observer.

III. ANALYSIS OF DATA

A. Minus-plus Ratio

The ratio of the number of π^- mesons to the number of π^+ mesons produced in a certain meson energy range is, simply:

$$\frac{\pi^-}{\pi^+} = \frac{1.37 \sigma}{\pi-\mu}$$

where σ and π - μ represent the number of σ and π - μ endings, respectively, found in a volume of emulsion corresponding to the energy in question.

There is another analytical method for determining the minus-plus ratio which is a less reliable method but is of interest to indicate experimental consistency. The method is developed as follows. The number of π^- mesons is again taken as 1.37σ . Since only π mesons are emitted from the target, the

-15-

difference between the total number of mesons, T , including ρ -types, and the number of π^- mesons, is due to π^+ and μ^+ mesons. Taking $\pi^+ = \mu^+$, it follows that

$$\left(\frac{\pi^-}{\pi^+}\right)_{\text{alternate}} = \frac{1.37 \sigma}{\frac{1}{2}(T - 1.37 \sigma)} = \frac{2}{0.73 \frac{T}{\sigma} - 1}$$

B. Energy Spectrum

For a point source emitting $\frac{d^2 N_0(E, \theta)}{dE d\Omega}$ π mesons per unit beam exposure per Mev per steradian at polar angle, θ , and with kinetic energy, E , it can be easily shown that

$$\left[\frac{d^2 N_0(E, \theta)}{dE d\Omega}\right]_{\text{av.}} = \frac{1}{Q} \frac{n}{\left(\frac{1}{R^2} \frac{dE}{dR}\right)_{\text{av.}}}$$

where:

n = the number of mesons ending per unit volume of the emulsion

Q = the number of "equivalent quanta"

R = distance from detector to source

dE/dR = the rate of energy loss in the emulsion evaluated at the energy E .

Since these quantities may vary over a large detection volume element, the indicated average must be taken over the detector.

One possible effect that might distort the emission spectrum as measured in this way is π - μ decay in flight; however, the time of flight^{16,17,18,19} in the air between the carbon target and the absorbing medium plus the slow down time in the absorber is so short that only about 3 percent of the π mesons

¹⁶ J. R. Richardson, Phys. Rev. 74, 1720 (1948)

¹⁷ E. Martinelli and W. Panofsky, Phys. Rev. 77, 465 (1950)

¹⁸ Kroushaar, Thomas, and Henri, Phys. Rev. 78, 486 (1950)

¹⁹ O. Chamberlain, R. Mozely, J. Steinberger, and C. Wiegand, Phys. Rev. 79, 394 (1950)

decay before coming to rest.

Another distorting effect is the nuclear scattering and absorption of the mesons while traversing the absorber. Indications are that the nuclear absorption cross section for mesons of energies greater than 150 Mev may be as great as a nuclear area,²⁰ in which case the absorption could be as much as 30 percent. Information on low energy mesons of about 30 Mev indicates that the nuclear absorption cross section may be somewhat less than a nuclear area but that the nuclear scattering cross section may be of the order of a nuclear area.²¹ The nuclear scatters of large angles would cause mesons of energy, E , to be detected at a position in the emulsions which corresponds to a smaller energy.

The measured emission spectrum could be distorted also if the approximation of a point source were not valid. However, calculations show that the point source approximation was justified for the target used.

In order to find out whether any of the mesons observed might have come from sources other than the carbon target a blank run was made, i.e., a run identical to the main run except that the carbon target was omitted. No mesons at all were found in areas which in the main run would have yielded about 130 mesons.

C. Cross Section

If one assumes the existence of some functional relationship between E , θ , and k , where k is the energy of the photon creating the meson of energy E at angle θ , one can relate the emission spectrum to the differential cross section

²⁰ U. Camerini, P. H. Fowler, W. O. Lock, and H. Muirhead, Phil Mag. 41, 413 (1950)

²¹ H. Bradner and B. Rankin, Phys. Rev. (to be published)

-17-

$$\frac{d\sigma(k, \theta)}{d\Omega} = \frac{d^2 N_0(E, \theta)}{dE d\Omega} \left(\frac{\partial E}{\partial k} \right)_\theta \frac{1}{V n_t \bar{N}(k)}$$

where:

\bar{N} = the integrated number of photons of energy k per Mev per unit beam exposure per square centimeter of beam area averaged over the volume, V , of the carbon target

$\frac{d\sigma(k, \theta)}{d\Omega}$ = cross section for the production of mesons per steradian at angle θ by a photon of energy, k , in cm^2 per nucleus

n_t = the numerical density of target atoms in cm^{-3} .

However, the correct model by which to calculate $\left(\frac{\partial E}{\partial k} \right)_\theta$ is not known, so that the above cross section was not computed. A cross section that can be computed without reference to any particular collision model is the mean cross section per steradian averaged over the x-ray energy spectrum. Integrating the meson spectrum we get:

$$\frac{d \overline{\sigma(\theta)}}{d\Omega} = \frac{dN_0(\theta)}{d\Omega} \frac{1}{Q n_t V}$$

where $\frac{dN_0(\theta)}{d\Omega}$ is the total number of mesons per steradian emitted at angle θ . The integrated number of photons, Q , per unit beam exposure per square cm of area, as used here is not clear cut. As a first approximation, for a bremsstrahlung beam one may write $\bar{N}(k) = A/k$ so that

$$Q = A \ln k_2/k_1$$

where k_1 and k_2 are the minimum and maximum effective photon energies, respectively.

Another method which avoids the approximation in the $1/k$ spectrum and a

-18-

knowledge of the threshold is to define the number of "equivalent quanta" as the total energy in the beam divided by the maximum photon energy. Then

$$Q = 1/k_{\max} \int_0^{k_{\max}} k \bar{N}(k) dk$$

If the actual bremsstrahlung spectrum has the shape $\bar{N}(k) = A/k$, this definition defines the total number of "equivalent quanta" as the constant, A.

From the ionization chamber, which was calibrated by Blocker, Kenney, and Panofsky²² by a method previously reported by them,²³ the total energy of the beam was obtained. From this energy measurement and the maximum photon energy of 322 Mev, the number of "equivalent quanta" was found.

The total cross section, $\bar{\sigma}_t$, may now be obtained by integrating the differential spectrum over all angular space:

$$\bar{\sigma}_t = 2\pi \int_0^\pi \frac{d\bar{\sigma}(\theta)}{d\Omega} \sin \theta d\theta$$

$\frac{d\bar{\sigma}(\theta)}{d\Omega}$ was measured at 3 angles, 45°, 90°, and 135°, so that extrapolation was necessary below 45° and above 135°. Fortunately, however, the $\sin \theta$ factor minimizes the effect of errors in these regions.

IV. RESULTS

A. Minus-plus Ratio

The ratios of the number of π^- mesons to the number of π^+ mesons in each energy interval for the three values of the angle θ are shown in Fig. 5.

The theoretical ratio for photon-nucleon collisions as determined by Brueckner

²² W. Blocker, R. Kenney, and W. K. H. Panofsky, private communication

²³ W. Blocker, R. Kenney, and W. K. H. Panofsky, Phys. Rev. 79, 419 (1950)

and Goldberger^{24,25} for the case in which the nucleon interacts only in the proton state is plotted in the same figure. The Coulomb effect of distributed charge has also been included.

Since, at each of the three angles observed, the experimental data are statistically consistent with a constant value of the minus-plus ratio as a function of energy, the data were combined to determine the overall minus-plus ratio at each angle. These values are given in Table II, along with the mean theoretical values found by weighting the theoretical value at each energy interval with the number of mesons found in that interval. The mean energy determined similarly is also listed. The alternate, less reliable, method of computing the minus-plus ratio, discussed in Section III-A, which uses the total number of mesons, was applied also to the data for the purpose of comparing the methods. It should be added that if one plots and integrates the negative and positive energy spectra separately and thus obtains the minus-plus ratios, the results agree well with those obtained by considering the ratio to be independent of energy.

TABLE II

Overall Minus-plus Ratio Versus Angle of Emission

Angle	Experimental Ratio	Weighted Theoretical Ratio	Mean Energy	Experimental Ratio (Alternate Method)
45°	1.29 ± 0.22	1.25	70 Mev	1.60
90°	1.30 ± 0.12	1.62	56 Mev	1.60
135°	1.34 ± 0.20	2.12	54 Mev	1.32

²⁴ K. A. Brueckner and M. L. Goldberger, Phys. Rev. 76, 1725 (1949)

²⁵ K. A. Brueckner, Phys. Rev. 79, 641 (1950)

The experimental ratio appears to be independent of angle, as well as energy, whereas the theoretical ratio is not. This result might be explained by scattering of the mesons before they escape the carbon nuclei in which they are formed. This effect would make all characteristics of the emission spectrum isotropic. However, this explanation does not hold as the experimental energy spectra do depend on angle of emission. Another possible explanation, as indicated in Brueckner's analysis,²⁵ is that the assumption of negligible photon interaction with the nucleon in the neutron state is not valid, but that the neutron does interact with electromagnetic field of the photon through its magnetic moment and does play an appreciable part in the process.

A previous experiment gave an overall ratio of 1.7 ± 0.2 at an angle of 90° .² That experiment differed from the present one, chiefly, in two respects; (1) a line target was used and (2) the angular resolution was only about $\pm 45^\circ$. The discrepancy between the old and new results is slightly greater than that allowed by the statistical errors; however, the new result is believed to be the more reliable, because of the greater experience of the observers.

B. Energy Spectra and Cross Sections

The spectra of π mesons emitted from the carbon target were computed from the data using the total number of π mesons, both positive and negative, at each energy interval. That is, it was assumed that the minus-plus ratio was independent of energy, as indicated in the last section. If one actually plots the negative and positive spectra separately, no statistically significant distinction appears in their relative shapes.

The emission spectra for 45° , 90° , and 135° are shown in Figs. 6, 7, and 8, respectively. Smooth curves were drawn through the experimental points and extrapolated to zero energy for the purpose of obtaining the total number

-21-

of mesons emitted at each direction. The dashed curves show the emission spectra corrected for nuclear absorption in the absorbers. A cross section of one nuclear area, as calculated from 90 Mev neutron cross section experiments,²⁶ was assumed. In Fig. 9 the three smooth curves are drawn together for the purpose of intercomparing the three spectra.

Integrals of the spectra lead to values of the average cross section per steradian listed in Table III.

TABLE III

Average Cross Sections per Steradian.

Emission Angle	$\overline{d\sigma}/d\Omega$ cm ² per steradian per nucleus per "equivalent quantum"
45°	$2.52 \pm 0.22 \times 10^{-29}$
90°	$3.87 \pm 18 \times 10^{-29}$
135°	$2.82 \pm 0.19 \times 10^{-29}$

The errors listed are purely statistical errors. There is also a systematic error of about ± 35 percent due to an uncertainty in the absolute calibration of the number of quanta in the beam, but it does not affect the relative validity of the cross sections given. The present calibration of the beam is good to about 10 percent;²² however, at the time the carbon exposures were made, the monitoring technique was not as reliable as at present.

The lack of a strong forward peak which would be predicted by classical electromagnetic theory if the interaction were that of an electric dipole effect has already been pointed out⁵ in a study of π^+ mesons produced by photons on hydrogen. The binding apparently plays a role in the shape of the

²⁶ L. J. Cook, E. M. McMillan, J. M. Peterson, and D. C. Sewell, Phys. Rev. 75, 7 (1949)

-22-

energy spectrum of carbon as results at 90° indicate that the hydrogen spectrum is considerably flatter than that of the carbon.

The effect of the binding of the nucleons is evidenced most strongly in the magnitude of the cross section. Comparison of these results at 90° with those of Cook⁴ from liquid hydrogen shows that the cross section per proton in the carbon nucleus for the production of π^+ mesons from carbon is only about 1/3 that from hydrogen. This result checks a previous result of Steinberger and Bishop.⁵

The cross section figures per steradian listed in Table II are also plotted in Fig. 10. The smooth curve in the figure was drawn in to obtain the total average cross section integrated over all angles. The resultant figure is 4.0×10^{-28} cm² per nucleus per "equivalent quantum." If the effect of nuclear absorption of the absorbers were included, again assuming an absorption cross section of one nuclear area, the total cross section for production of mesons would be increased by 30 percent. The total uncertainty in the cross section is due largely to the uncertainty in the absolute calibration of the beam in terms of the monitor used and is estimated to be about ± 40 percent.

C. Internal Consistencies

The angular distributions of the mesons found at the emission angle of 90° are plotted in Fig. 11. The angle of each meson is measured at the point where it enters the emulsion. The projected track lengths in emulsion ranged from 25 to 4000 microns, but the bulk of them lay in the 100 to 200 micron interval, as shown in Fig. 12. Choosing mesons which end near the middle of the various plates with residual ranges of 200 microns as typical, one finds that the calculated r.m.s. angle of scatter varies from 14° to 21° over the energy range covered

-23-

and is in the neighborhood of 18° where most of the mesons were found. Both the σ -meson and the π - μ meson plots of Fig. 11 give half widths of 17.5 degrees at half amplitude in good agreement with the calculated amount of multiple scattering.

The distribution of the angles at which the μ^+ mesons leave the end of the π^+ mesons, measured with respect to the beam direction, is clearly isotropic within the statistics involved. That the μ^+ mesons are isotropic also with respect to the angle to the normal to the emulsion plane is shown by the track length distribution of the μ^+ mesons in Fig. 12. The smooth curve is the calculated curve for isotropic emission from points uniformly distributed throughout the scanned volume.

The plot of the angular distribution of the ρ mesons is clearly composite, being composed of a peak at 90° due to π^- mesons which do not make stars and a flat background due to μ^+ mesons whose beginnings are not observed. One can find the fraction of π^- mesons which do not form stars by comparing the number of mesons under the hump of the ρ meson plot, after subtracting off the flat background, with the number of σ mesons on the plot above. This fraction turns out to be 0.31 ± 0.07 , the error being purely statistical. This value compares well with the value 0.27 ± 0.02 found by Adelman and Jones⁹ with magnetically sorted negative mesons. The angular width of this hump is again about 17.5 degrees.

If μ mesons were formed in the target they would appear as ρ mesons in the plates and would contribute to the hump in the ρ meson angular distribution. If the value 0.27 is used as the real fraction of the π^- mesons which do not form visible stars, one can again use the number of ρ mesons in the hump to determine an upper limit on the cross section for the production of μ mesons. By subtracting from this group of ρ mesons 0.27 times

-24-

the total number of π^- mesons, as determined by the number of σ mesons in the same angular range, one obtains a residual number of ρ mesons possibly attributable to μ mesons from the target. Assuming that the μ mesons are produced in pairs, one arrives at an upper limit to the ratio of the cross section for μ meson production to that for π meson production. This value is 0.02 ± 0.02 ; the error is statistical.

The angular plots for emission angles of 45° and 135° correspond very well with those obtained at 90° but are less conclusive as fewer mesons were counted there.

It is a pleasure to acknowledge the continued guidance and support of Professor E. M. McMillan. We wish to thank Mrs. Edith Goodwin and Mrs. Hazel Gaffey for help in the microscope work, Drs. H. Bradner, E. Gardner, and co-workers for the use of the facilities of the Radiation Laboratory Film Program and for many helpful discussions, Mr. W. Salsig for mechanical design, and Mr. W. D. Gibbins and the other members of the synchrotron crew for cooperation in making the exposures.

This work was performed under the auspices of the Atomic Energy Commission.

Information Division
scb/10-17-50.

Figure Captions

- Fig. 1: Schematic drawing showing the essential experimental components.
- Fig. 2: A. Drawing of a longitudinal view of the collimator-target-detector assembly.
B. Drawing of a cross sectional view of the target-detector assembly.
- Fig. 3: Photograph of the experimental arrangement. The x-ray beam emerges from the synchrotron at A. B is the primary lead collimator. C is the copper absorber. Copper boxes containing the nuclear plates fit into the longitudinal slots. The x-ray beam emerges from this assembly at D.
- Fig. 4: Depth distributions of the three types of mesons found. Data from all angles are included.
- Fig. 5: Plots of the experimental minus-plus ratio against meson energy for three angles of emission. The theoretical curve is for the case in which the neutron-photon interaction is negligible; the Coulomb effect of a distributed charge is included.
- Fig. 6: Experimental energy spectrum of π^- and π^+ mesons emitted at 45° to the beam direction in units of 10^{-8} mesons per Mev per steradian per "equivalent quantum." The smooth curve through the data has been drawn for purposes of integration. The dotted line below 30 Mev has been extrapolated. The dashed curve shows the emission spectrum corrected for nuclear absorption in the absorber. The cross section for absorption was assumed to be one nuclear area.
- Fig. 7: Experimental energy spectrum of π^- and π^+ mesons emitted at 90° to the beam direction in units of 10^{-8} mesons per Mev per steradian per

"equivalent quantum." The smooth curve through the data has been drawn for purposes of integration. The dotted line below 30 Mev has been extrapolated. The dashed curve shows the emission spectrum corrected for nuclear absorption in the absorber. The cross section for absorption was assumed to be one nuclear area. The indicated error for the point with zero ordinate was taken as that due to one meson.

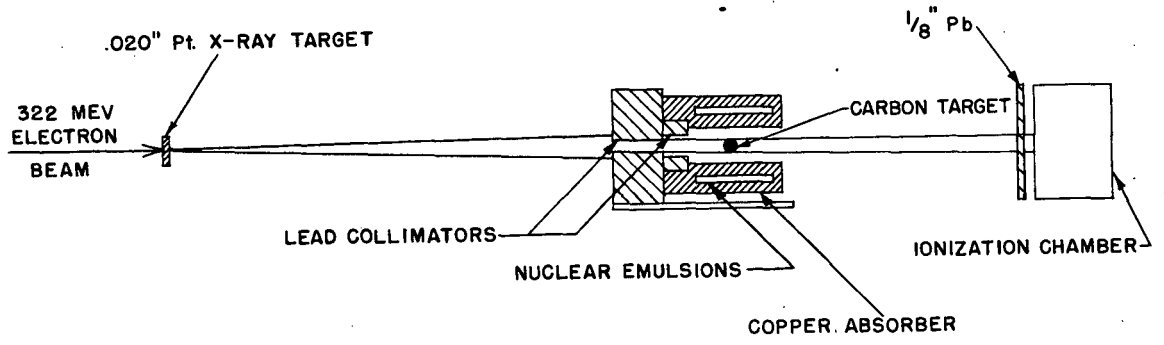
Fig. 8: Experimental energy spectrum of π^- and π^+ mesons emitted at 135° to the beam direction in units of 10^{-8} mesons per Mev per steradian per "equivalent quantum." The smooth curve through the data has been drawn for purposes of integration. The dotted line below 30 Mev has been extrapolated. The dashed curve shows the emission spectrum corrected for nuclear absorption in the absorber. The cross section for absorption was assumed to be one nuclear area.

Fig. 9: An intercomparison of the three energy spectra. These are the curves which were not corrected for nuclear absorption.

Fig. 10: Average π meson cross section per carbon nucleus per "equivalent quantum" in units of 10^{-29} cm^2 per steradian. The smooth curve was drawn for the purpose of integration. The dashed curve shows the cross section corrected for nuclear absorption in the absorber. The cross section for absorption was assumed to be one nuclear area.

Fig. 11: Angular distributions of the mesons found at 90° . The abscissa is the angle from the beam direction.

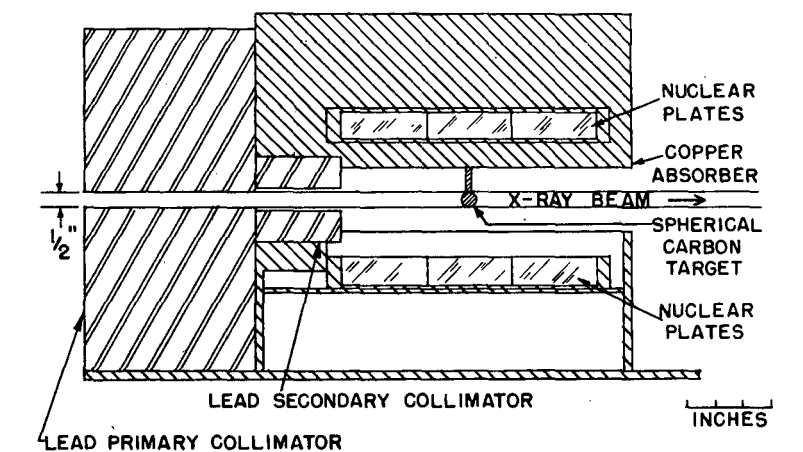
Fig. 12: Distributions in projected track length in emulsion for four types of mesons. Data from all angles included. The track length measurements are estimated to be accurate to within 10 percent.



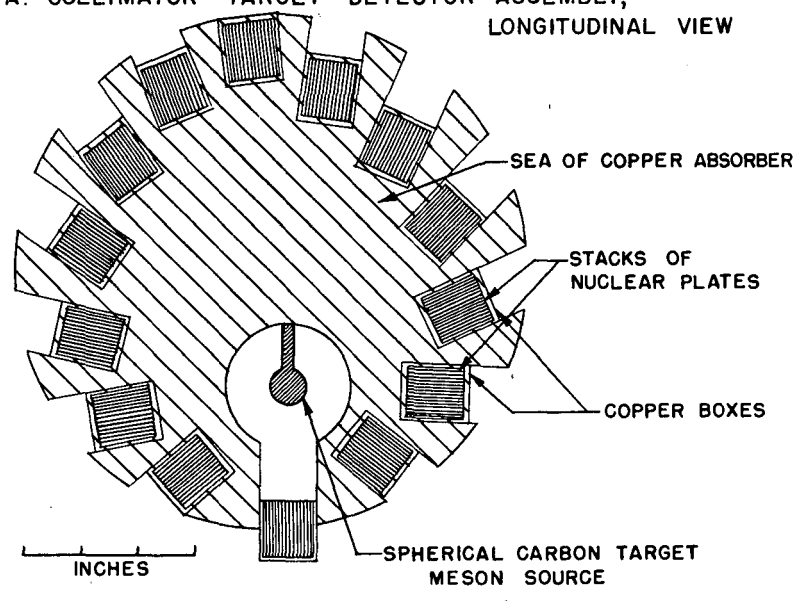
EXPERIMENTAL ARRANGEMENT

MU 923

Fig. 1



A. COLLIMATOR - TARGET - DETECTOR ASSEMBLY, LONGITUDINAL VIEW



B. TARGET - DETECTOR ASSEMBLY, CROSS SECTION VIEW

MU 925

Fig. 2

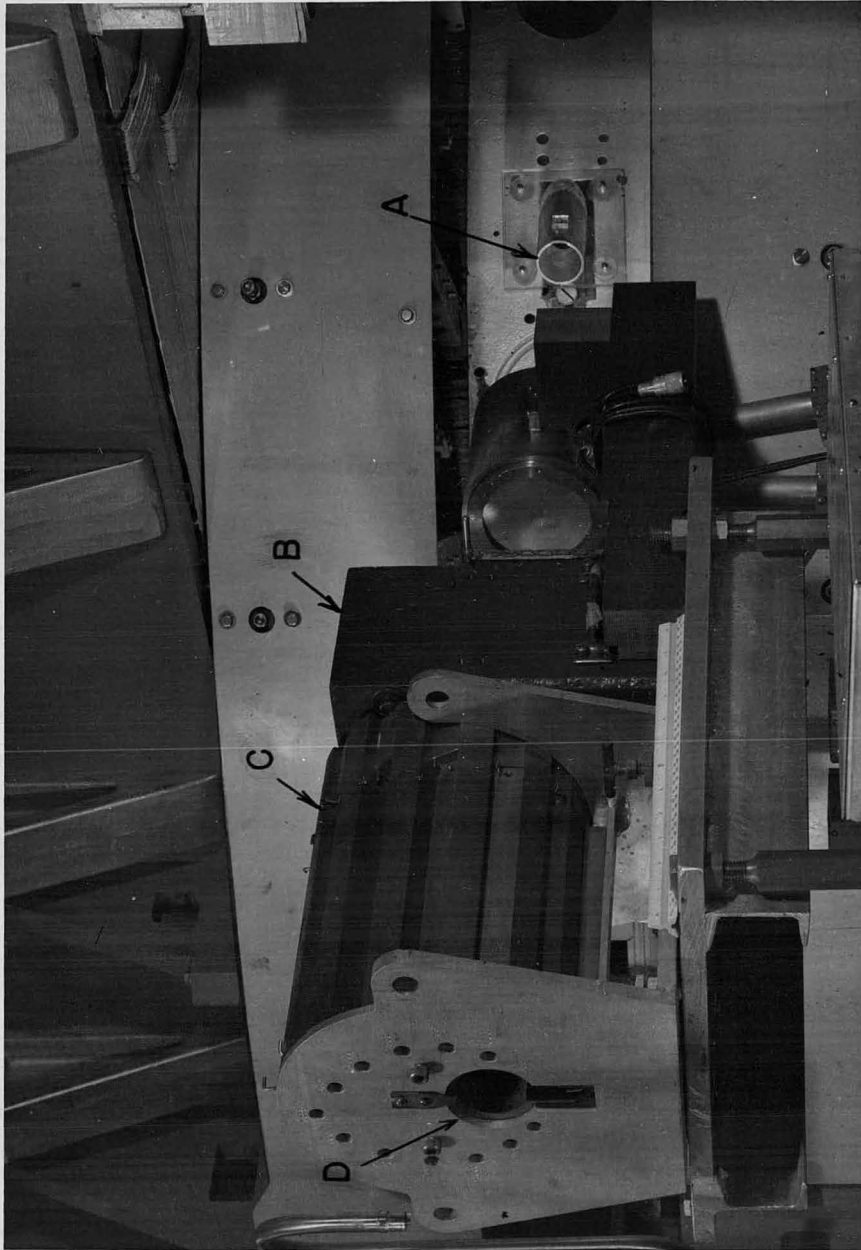
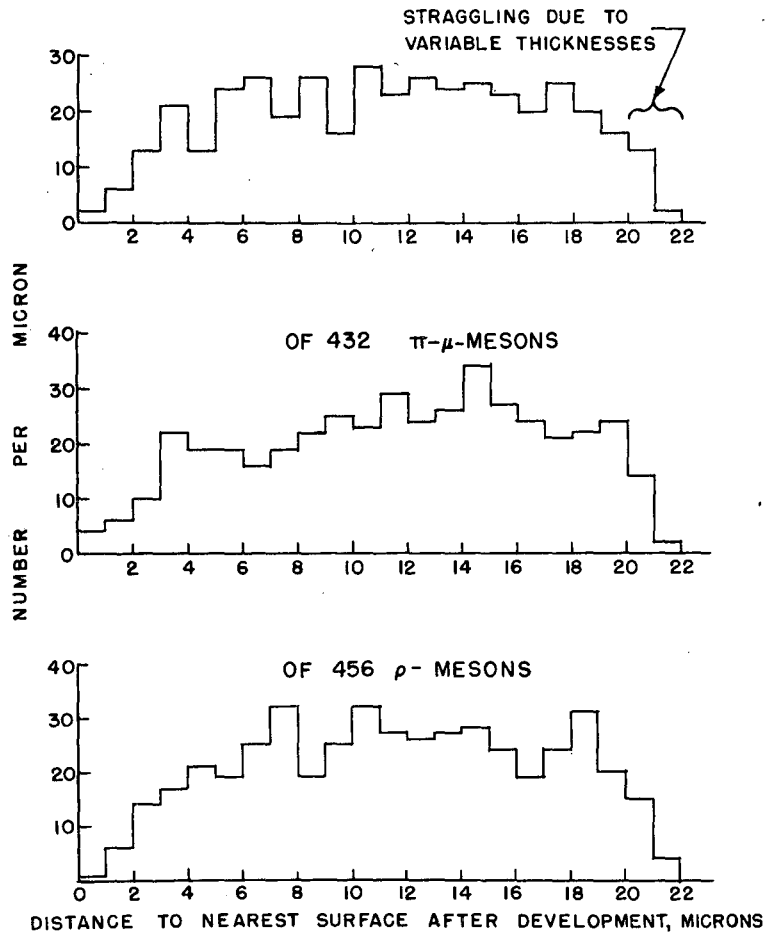


FIG. 3

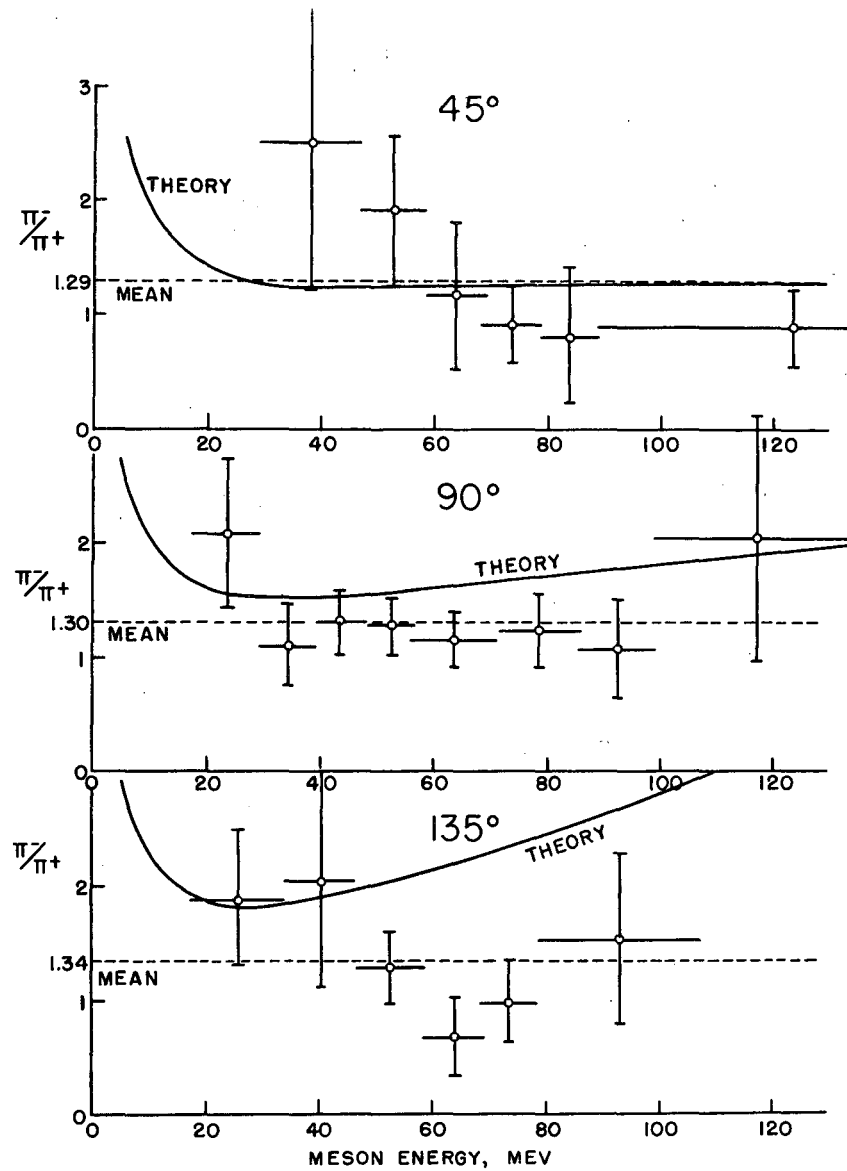
DEPTH DISTRIBUTIONS

OF 411 σ -MESONS



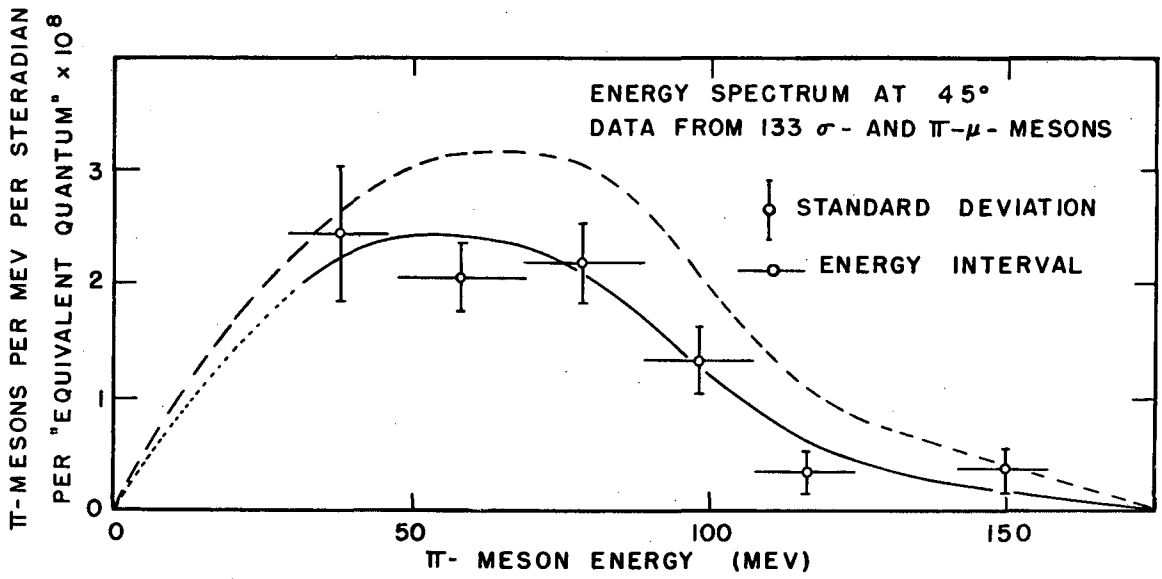
MU 922

Fig. 4



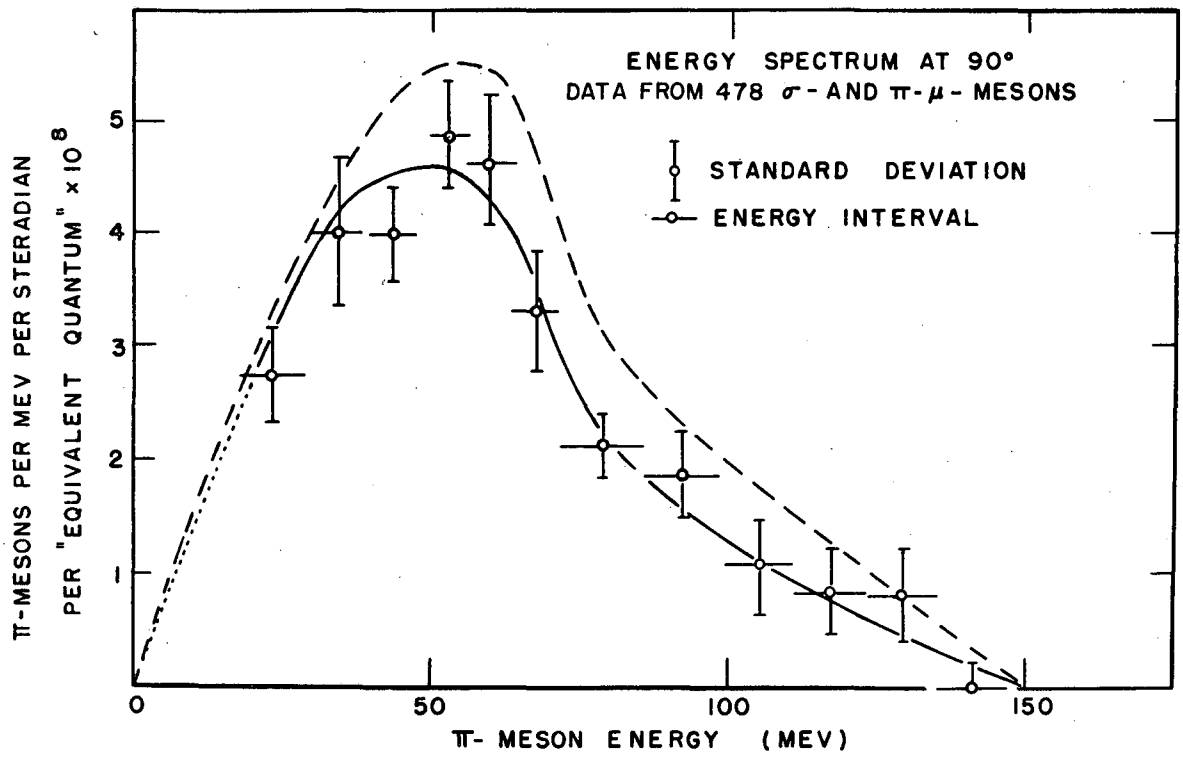
MU 924

Fig. 5



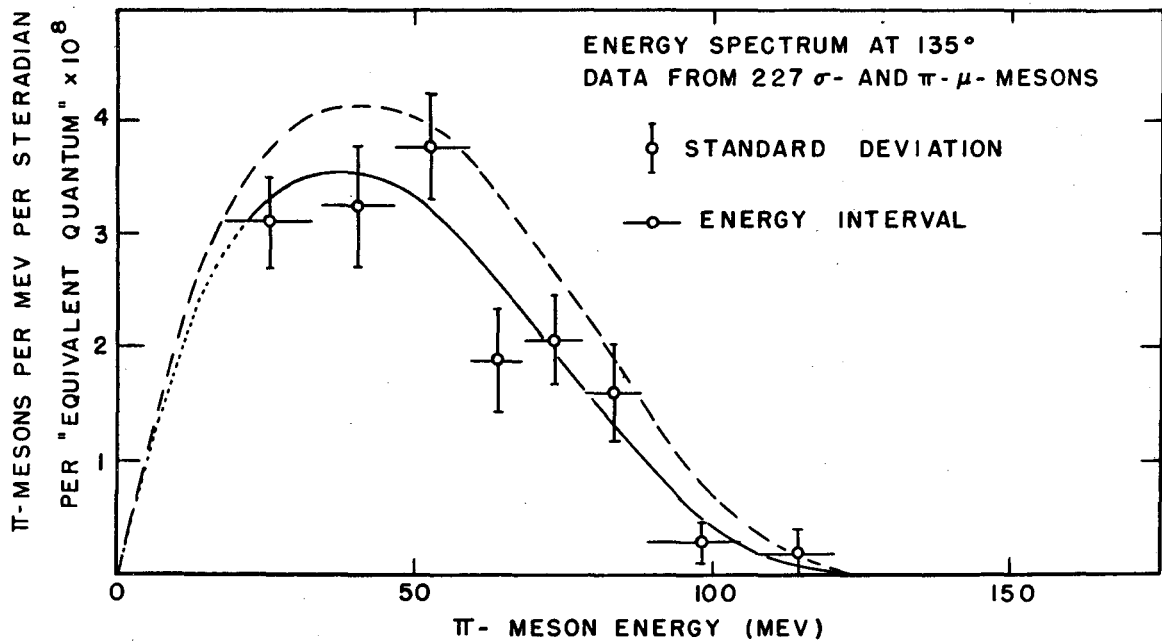
MU 915

Fig. 6



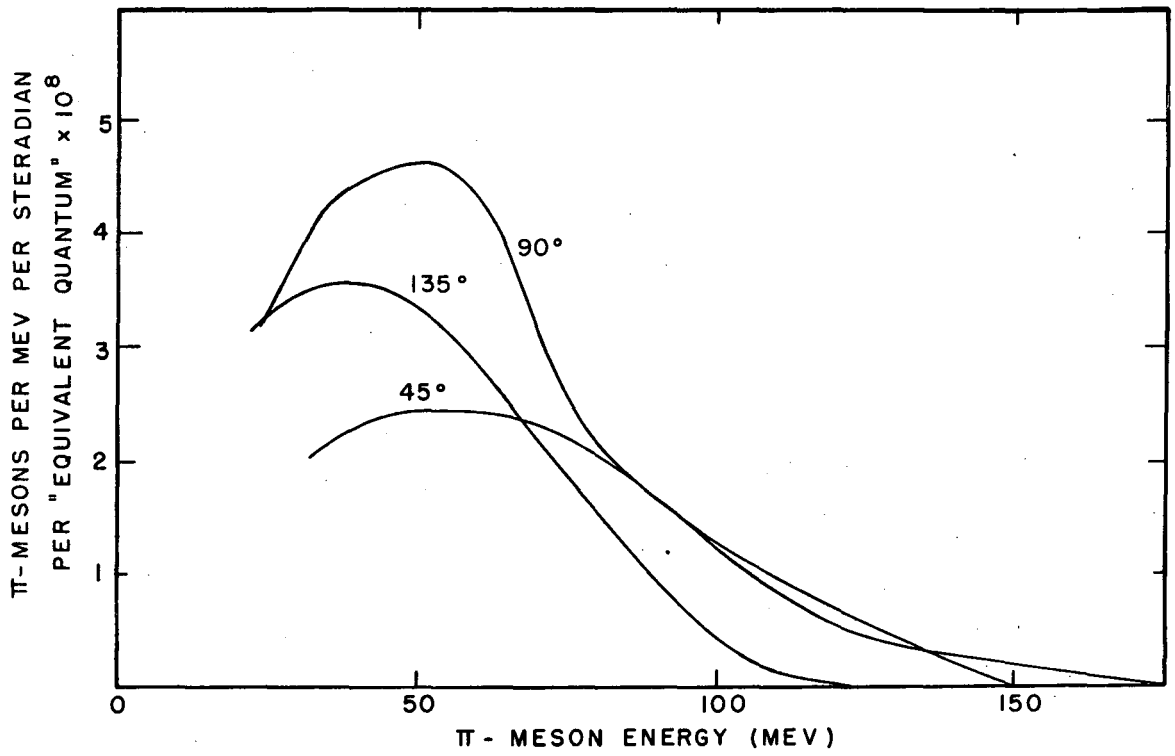
MU 917

Fig. 7



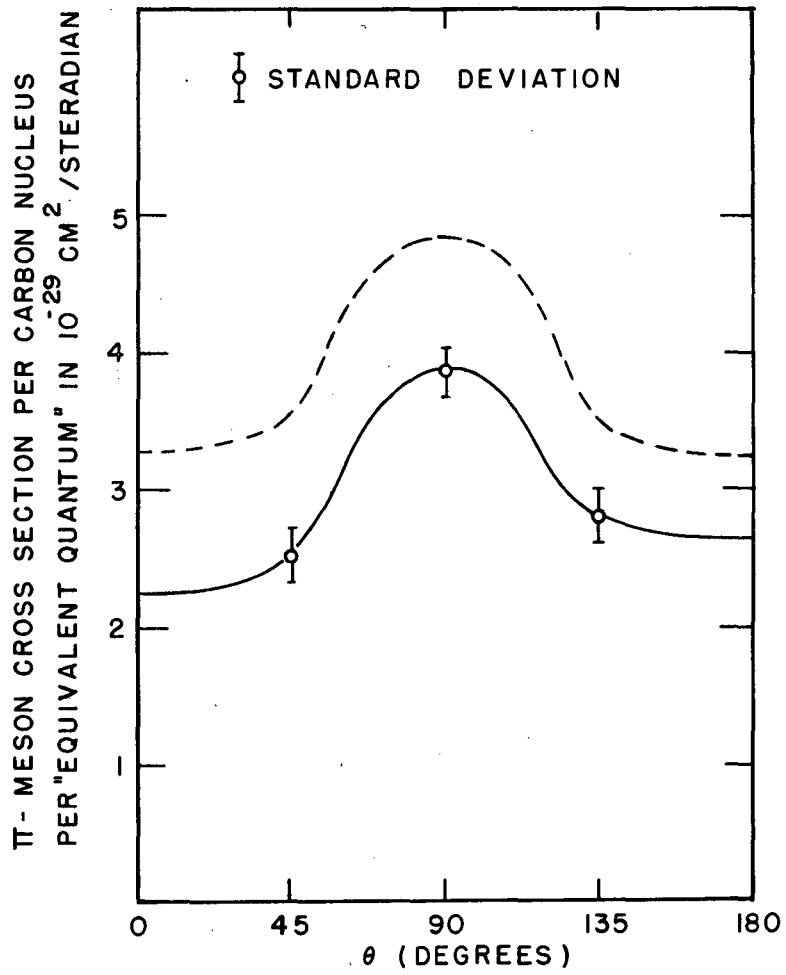
MU 916

Fig. 8



MU 918

Fig. 9



MU 919

Fig. 10

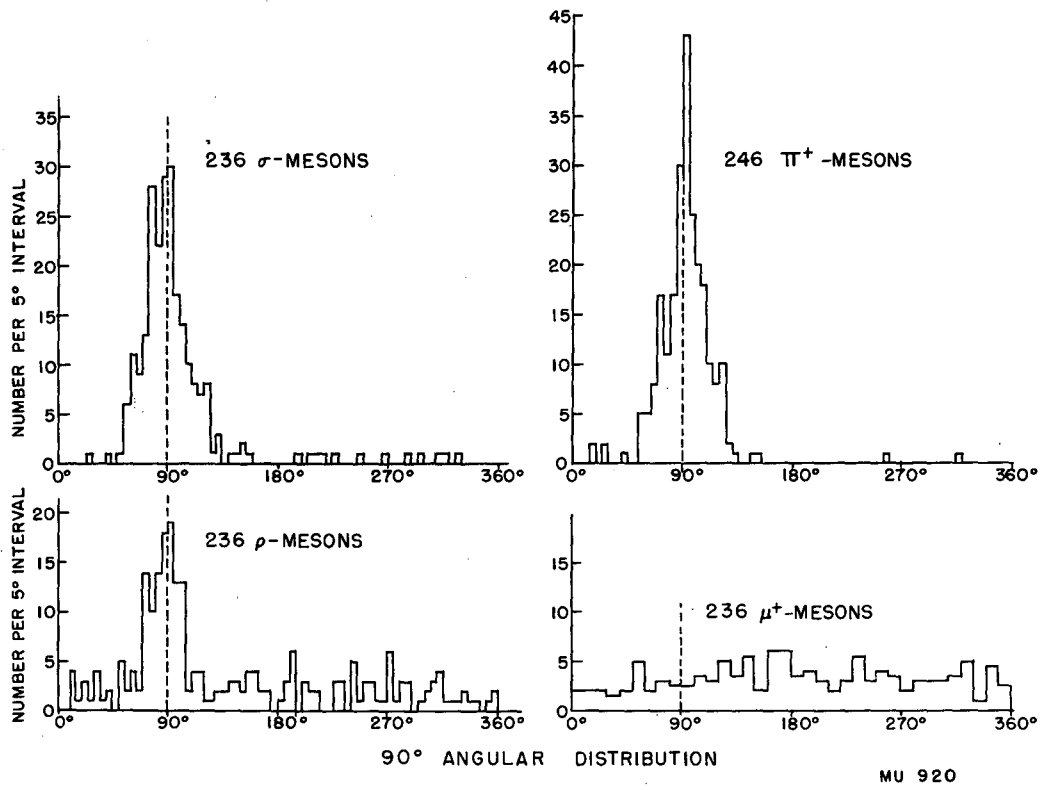


Fig. 11

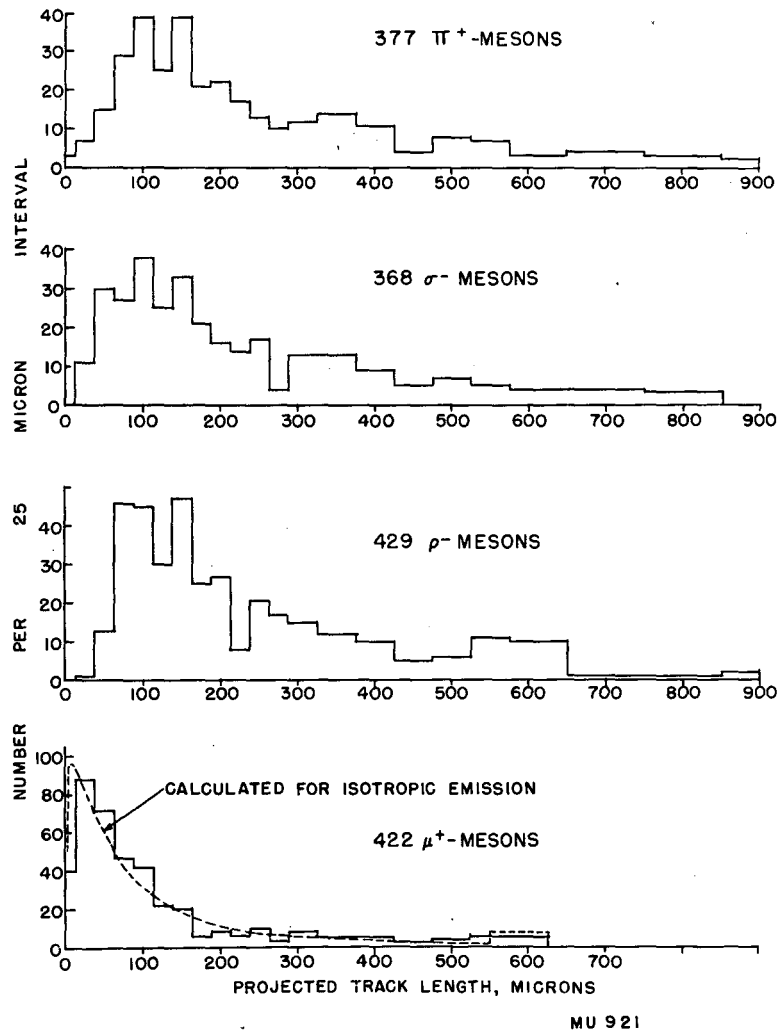


Fig. 12